

Supercritical Methane Diffusivity in Porous Media

Nicholas J. Drenzek^{‡*}, Prem K. Bikkina[†], Jarred H. Kelsey[†], Clint P. Aichele[†], Jeffery L. White[†]

[‡]BHGE Oil & Gas Technology Center, Oklahoma City OK 73104 USA

[†]Oklahoma State University, Stillwater OK 74078 USA

This paper was prepared for presentation at the International Symposium of the Society of Core Analysts held in Trondheim, Norway, 27-30 August 2018

ABSTRACT

The self-diffusion coefficients and transverse relaxation rates of supercritical methane at temperatures and pore pressures up to 60°C (140°F) and 62.1MPa (9000psig) were measured in sandstone (SS) and limestone (LS) microplugs at dry and irreducible brine saturation in zirconia tubes using 400MHz nuclear magnetic resonance (NMR) spectroscopy. Diffusivities in the tube annuli, whose 0.3mm apertures approximate that of subsurface fractures, were on the order of $10^{-8}\text{m}^2\text{s}^{-1}$. These values were up to three times higher than those in the network of pores, whose volume-distributed mode CT-derived diameters were 35 and 5 μm for SS and LS respectively. All diffusion coefficients decreased exponentially by a factor of 2-3 from 13.8 to 62.1MPa in SS and LS, and all decreased by a factor of 1-3 across an 8 to 64ms increase in echo spacing. Corresponding annular and pore relaxation rates generally increased with pressure from 42 to 139 and 37 to 71ms for SS, and 46 to 144ms and 90 to 217 for LS, respectively. These trends compare reasonably well against quantitative model predictions of the progressive disruption of spin-rotation proton relaxation with increasing pressure.

INTRODUCTION

The pore pressure of fluids in petroleum reservoirs fundamentally controls storage and flow therefrom via its regulation of advection and phase separation. It also impacts operational safety e.g. mud weight, well kicks, and blowouts, which has underpinned interest in development of ahead-of-bit, logging-while-drilling pore pressure sensors. Real time, *in situ* determinations based on acoustic, nuclear, and electric modalities are all beset by their sensitivities to other formation properties such as rock and fluid composition, and thus rely on semi-quantitative analysis of trends with depth.

Reservoirs that are most prone to spontaneous pressure drives for production and safety operations, i.e. those that are deep, mature, gas-filled or gas-capped, overpressured, and millidarcy permeable, are also endowed with other petrophysical properties, e.g. abundant, large (low S/V) pores within a ferromagnetic-lean mineral framework, that lend them to interrogation by nuclear magnetic resonance (NMR), which has been shown to be sensitive to pressure [1, 2, 3, 4] through the pressure dependence of the Brownian-

motion portion of nuclear spin relaxation. On the micro- to millisecond timescale of a NMR radiofrequency pulse-echo measurement, ballistic Brownian motion can be approximated as diffusion, and it contributes to the rate of NMR transverse spin-rotation relaxation in gases and supercritical fluids by changing the frequencies of intermolecular collisions and dipole coordinations, respectively [4, 5]. As pressure increases, both interactions become less frequent, decreasing the transverse relaxation rate (and increasing the corresponding T2 relaxation time constant). In non-advective, well-mixed, isothermal, single or multi-component fluids (such as in oilfield reservoirs before primary drainage or during enhanced oil recovery [EOR] soak periods), the decrease in the Brownian diffusion coefficient (D) and corresponding increase in T2 time can be encoded by modern NMR logging tools using a modified pulse-echo sequence [6].

The goal of this study was to ascertain the magnitude of these NMR signals attributable to Brownian diffusion alone in a simple lab-based analogy to subsurface applications. The spectral resolution afforded by high-field (400MHz) NMR was exploited to discriminate between bulk (i.e. fracture) and pore diffusion coefficients (D_B and D_P respectively) and transverse relaxation rates ($T2_B$ and $T2_P$) of supercritical methane within sandstone (SS) and limestone (LS) microplugs, which are good analogues for the spontaneous pressure driven reservoirs discussed above, under isothermal conditions over a range of reservoir-relevant pressures. The empirical responses were then compared against methane self-diffusion values calculated from elementary mean free path theory under environmental conditions prescribed by a simple subsurface model, which were in turn coupled with measured petrophysical characteristics to estimate the magnitude of the Brownian diffusion term in the NMR relaxation equation. Finally, these findings were extrapolated to oil and brine phases to determine if pressure-driven variations in their corresponding diffusion terms could be discriminated against variations in bulk and surface counterparts caused by other factors [7].

PROCEDURE

Experimental

Briefly, small microplugs (3mm O.D. x 10mm long, for high pressure high field [HPHF] NMR measurements) as well as standard plugs (4cm O.D. x 4cm long, for routine petrophysical property measurements) were recovered from samples of Kirby SS and Indiana LS, Soxhlet extracted using sequential toluene and methanol/chloroform azeotrope reflux, and allowed to fully dry at 104°C (220°F). Porosities (Φ_{CT}), volume-distributed mode pore diameters (d_{CT}), mean pore surface-to-volume ratios (S/V_{CT}), formation factors (FF_{CT}), cementation exponents (m_{CT}), tortuosities (τ_{CT}), and permeabilities (k_{CT}) were calculated by a binarization, distance-mapping, skeletonization, erosion, and expansion sequential workflow applied to GE Phoenix Nanotom 180 m microCT images acquired on 5x5mm (diameter x height) rinded end trims of the standard plugs at voxel edge resolutions of 1.5 μ m for SS and 2.0 μ m for LS. Boyle's law effective porosities (Φ_{He}) and pressure-decay Klinkenberg-corrected permeabilities (k_{He}) were measured by CoreLab CMS-300 on the standard plugs confined at 3.4MPa (500psig) and

41.4MPa (6000psig). Following vacuum saturation with a 20wt% potassium chloride brine solution, T2 distributions were determined from multi-exponential fit to 2MHz Maran Ultra NMR CPMG-induced echo trains with interecho spacing (t_E) = 0.20ms acquired on the standard plugs under STP conditions, which were in turn used to estimate effective porosities (ϕ_{NMR}), permeabilities (k_{NMR} using the SDR method), and when correlated to S/V_{CT} distributions, mean NMR surface transverse relaxivities (ρ_2) [8]. Electric formation factors (FF_e) were then measured at 81°C (178°F) and 1000Hz under 41.4MPa confinement against a bulk brine resistivity value of 0.020ohm-m, from which Archie cementation exponents (m_e) and electric tortuosities (τ_e) were calculated. Finally, methane-displacing-brine capillary pressure curves and irreducible brine saturations (S_{wi}) were measured on the standard plugs between 0-6.9MPa (0-1000psig) endmembers by centrifuge, the data from which was used to bring the matching microplugs (whose pore fluid volumes are too small to measure) to S_{wi} by centrifuge as well.

For each HPHF NMR experiment, a microplug was inserted into a Daedalus Innovations 100.0MPa (14500psig)-rated cylindrical (5mm O.D. x 3.6mm I.D. x 92mm long) zirconium NMR tube containing a small boron nitride spacer designed to elevate the microplug into the sensitive volume. The tube was then assembled into a Viton-sealed titanium needle valve manifold, purged several times with UHP 5.0 methane, pressurized with the same methane in a 60°C (140°F) convection oven using a Teledyne Isco 260 HP syringe pump to the first target pressure value of 13.8MPa (2000psig), sealed, and inserted into a 60°C thermostated diffusion probe within a Bruker Ascend 400MHz NMR for measurement. Pressures were sequentially increased to target values of 27.8, 41.4, 55.2, and 62.1MPa (4000, 6000, 8000, and 9000psig) between each measurement without venting the tube. D_B and D_P values were acquired for t_E = 8, 16, 32, 48, and 64ms at the lowest and highest pressures, while those at intermediate pressures were acquired for t_E = 16 and 64ms. Mean T_{2B} and T_{2P} values were acquired at t_E = 1ms at all pressures.

Model

D_B values of supercritical methane were calculated for 60°C for each experimental pressure using a quadratic fit with density, while those for 30° API oil and 20wt% brine were estimated for 60°C using the Einstein-Stokes approximation [9 and references therein]. D_P values for each fluid were then estimated by dividing by τ_{CT} . Corresponding T_{2P} values were calculated by the standard NMR equation (with bulk, pore, and diffusive terms) using the measured values of S/V_{CT} and ρ_2 , a t_E set at 1ms, and the mean experimental magnetic field gradient of $0.004T\text{ cm}^{-1}$, while T_{2B} counterparts were based on the annular S/V of the NMR tube.

RESULTS & DISCUSSION

Petrophysical properties measured by both traditional and digital (i.e. microCT-derived) methods generally agreed well (Table 1). The SS ρ_2 of $45\mu\text{m s}^{-1}$ is about twice as large than previously reported values up to $25\mu\text{m s}^{-1}$ [10] and might be attributable to either the (a) higher SS iron oxide content of 1.1wt% (versus 0.3wt% for LS) as determined by X-

ray fluorescence spectroscopy, or (b) skewed fit of the S/V_{CT} -derived T2 distribution to the low-field NMR counterpart arising from a broad, short-relaxing peak in the latter (data not shown). HPHF NMR downfield and upfield peaks were attributed to bulk and pore methane inventories respectively based on sharper peak shapes expected for bulk fluids as well as less shielding expected for pore fluids due to a combination of 3D volumetric averaging of surrounding paramagnetic effects [11] and minimized induction of counter-fields in small restricted pore volumes [12, 13].

Corresponding mean D_B , D_P , T_{2B} , and T_{2P} values were also in reasonable agreement with model predictions (Figure 2). Measured diffusivities decreased and transverse relaxivities increased by a factor of 2-3 across a fourfold increase in pressure (Figure 2). The generally lower values of LS D_B and T_{2B} versus their pore counterparts likely arise from fluids hosted in one more exceptionally large pores whose diameters exceed that of the annulus. Indeed, the microCT-derived pore size distribution for LS is 97% v/v dominated by a single 1.6mm wide vug (data not shown). The factor of ~ 3 model overestimated T_{2B} for both SS and LS is likely attributable to either errors in the S/V_{CT} and ρ_2 inputs or an unexpectedly high ρ_2 for the NMR tube itself.

Measured diffusivities decreased by a factor of 1-3, and the difference between those acquired at low and high pressure narrowed, across an eightfold increase in t_E (Figure 3). Since the mean displacement $\langle x \rangle$ of molecules with diffusivities $\sim 10^{-8} \text{m}^2 \text{s}^{-1}$ over an echo time of $\sim 10^{-2} \text{s}$ is about 10^{-5}m (i.e. of the same order as the SS and LS pore diameters), these results are consistent with an increasingly restricted path observed at longer timescales, and bound t_E to at least $\sim 30 \text{ms}$ for accurate diffusivity measurements at high pressure and $>64 \text{ms}$ at low pressure. Therefore, the actual D_B and D_P trends with pressure are likely to be even more shallow than reported here (i.e. Figure 2).

Subsurface application of these findings is bounded by the opposing effects of increasing temperature and pressure on reservoir fluid density [14], which in turn controls the aforementioned frequencies of NMR-relaxing intermolecular collisions and dipole coordinations. The density of supercritical methane will increase approximately twice as fast with the pressure gradient from top to bottom of a typical reservoir as it declines due to the corresponding temperature gradient, combining to yield a ca. 40% decrease (increase) in D_P (T_{2P}). And although abnormal pressure gradients would have a proportional effect, the absolute D_P and T_{2P} values reported herein currently confounds overpressure detection with extant low field NMR oilfield logging tools given their limited precision applied to reservoirs exhibiting intrinsically multimodal pore size and S/V distributions (which lead to broad D-T2 distributions). Extension of the model to the density of oil underscored its insensitivity to pressure, while the that of brine increased at a greater than threefold rate with temperature versus pressure.

CONCLUSION

HPHF NMR-enabled experimental observations of the decrease in Brownian diffusion and corresponding increase in transverse relaxivity of supercritical methane with increasing pressure were found to be in reasonable agreement with model predictions yet too modest for quantification by current downhole NMR technology.

ACKNOWLEDGEMENTS

This work was funded by the General Electric (GE) Company. Holger Thern and Oliver Mohnke (BHGE) contributed reviews that significantly improved the manuscript.

REFERENCES

1. Horch, C., S. Schlayer, and F. Stallmach, "High-Pressure Low-Field ^1H Relaxometry in Nanoporous Materials," *Journal of Magnetic Resonance*, (2014) **240**, 24-33.
2. Freedman, R., V. Anand, B. Grant, K. Ganesan, P. Tabrizi, R. Torres, D. Cantina, D. Ryan, C. Boreman, and C. Kruecki, "A Compact High-Performance Low-Field NMR Apparatus for Measurements on Fluids at Very High Pressures and Temperatures," *Review of Scientific Instruments*, (2014) **85**.
3. Papaioannou, A., and R. Kausik, "Methane Storage in Nanoporous Media as Observed via High Field NMR Relaxometry," *Physical Review Applied*, (2015), **4**, 2.
4. Lang, E.W., and H.-D. Lüdemann, "Density Dependence of Rotational and Translational Molecular Dynamics in Liquids Studied by High Pressure NMR," *Progress in NMR Spectroscopy*, (1993), **25**, 507-633.
5. Hubbard, P.S., "Theory of Nuclear Magnetic Relaxation by Spin-Rotational Interactions in Liquids," *Physical Review*, (1963) **131**, 3, 1155-1165.
6. Kärger, J., H. Pfeifer, and W. Heink, "Principles and Application of Self-Diffusion Measurements by Nuclear Magnetic Resonance," *Advances in Magnetic Resonance*, (1988), **12**, 1-89.
7. Kleinberg, R.L., and H.J. Vinegar, "NMR Properties of Reservoir Fluids," *The Log Analyst*, (1996), Nov-Dec, 20-32.
8. Kleinberg, R.L., 1999, "Nuclear Magnetic Resonance," *Experimental Methods in the Physical Sciences*, (1999), **35**, 337-377.
9. Hirasaki, G., S.-W. Lo, and Y. Zhang, "NMR Properties of Reservoir Fluids," *Magnetic Resonance Imaging*, (2003), **21**, 269-277.
10. Marschall, D., J.S. Gardner, D. Mardon, and G.R. Coates, "Method for Correlating NMR Relaxometry and Mercury Injection Data," SCA Conference Paper Number 9511, (1995), 1-12.
11. de Dios, A.C., and C.J. Jameson, "Recent Advances in Nuclear Shielding Calculations," *Annual Reports on NMR Spectroscopy*, (2012), **77**, 1-79.
12. Ok, S., D.W. Hoyt, A. Andersen, J. Sheets, S.A. Welch, D.R. Cole, K.T. Mueller, and N.M. Washton, "Surface Interactions and Confinement of Methane: A High Pressure Magic Angle Spinning NMR and Computational Chemistry Study," *Langmuir*, (2017), **33**, 1359-1367.

FIGURES

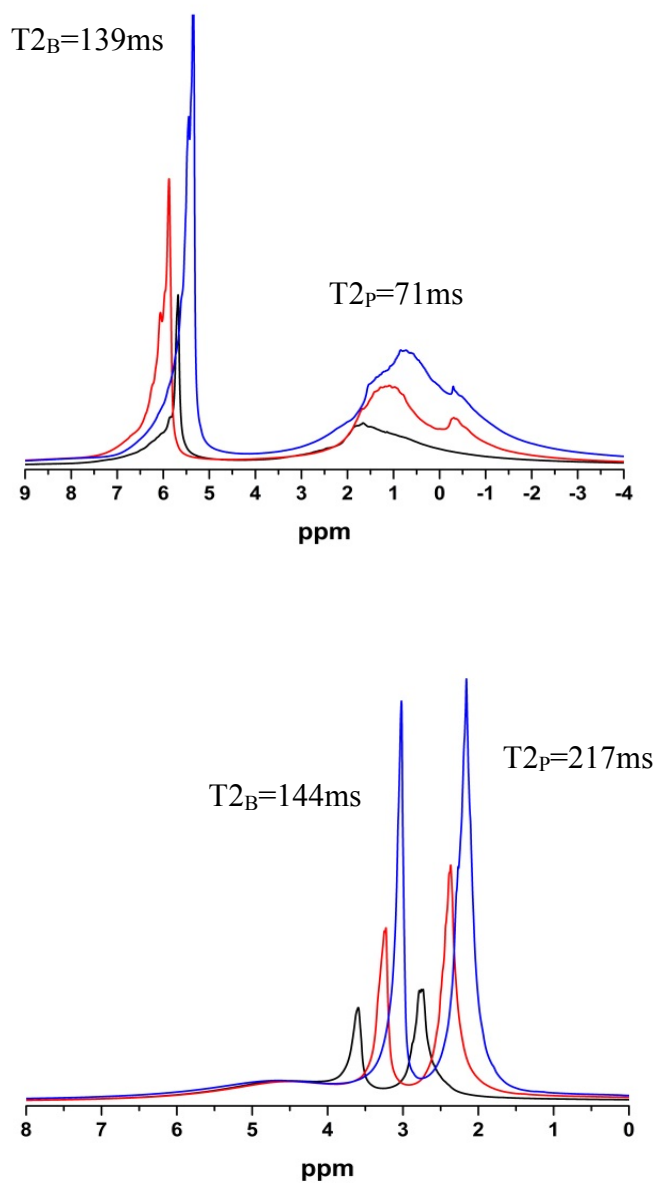


Figure 1 – HPFH NMR chemical shift spectra for SS (top) and LS (bottom) microplugs at 13.8 (black), 27.8 (red), and 62.1MPa (blue) along with T_{2B} and T_{2P} assignments at 62.1MPa.

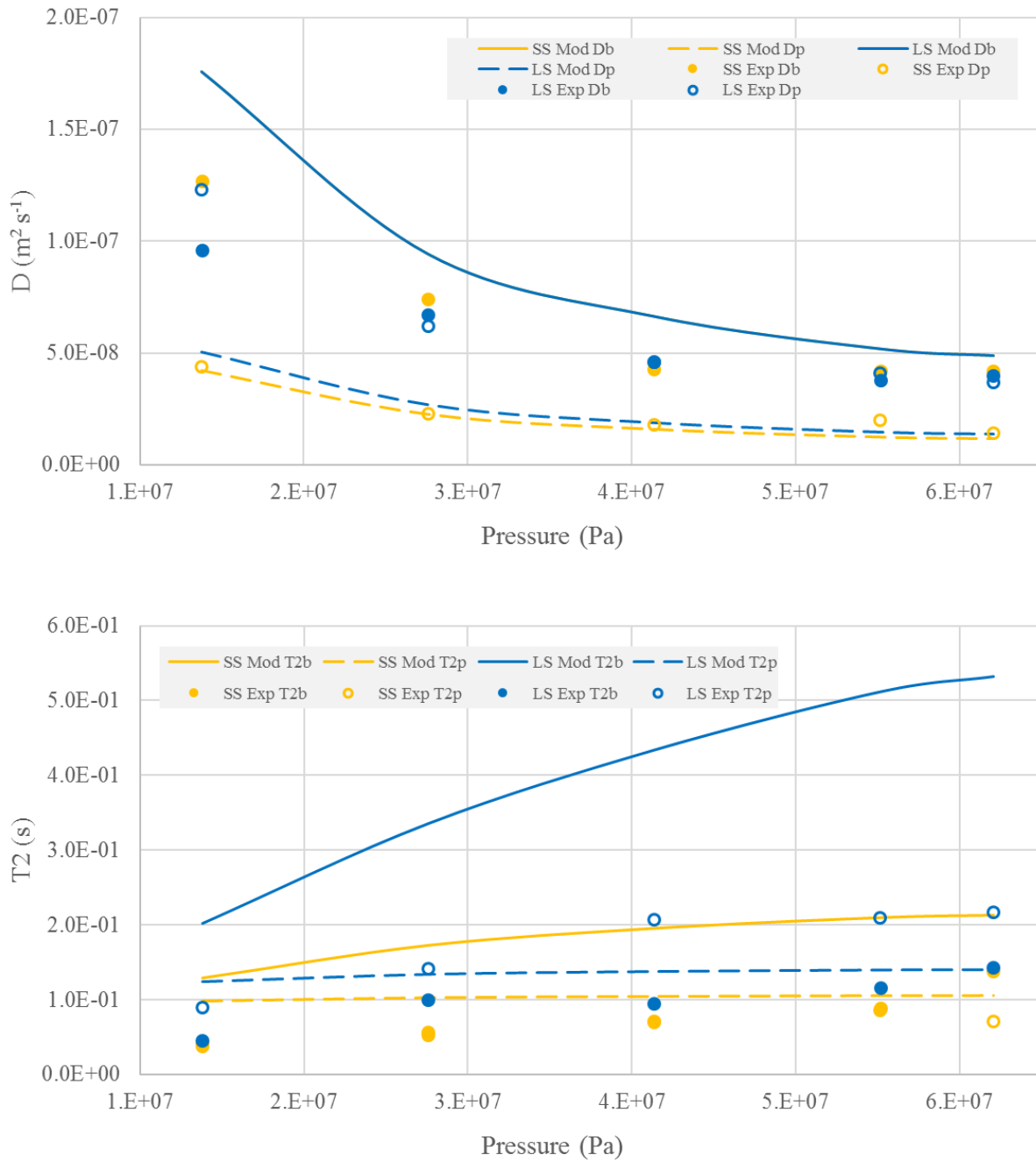


Figure 2 – Model predicted (‘Mod’) alongside experimentally determined (‘Exp’ at $t_E=64ms$) D_B , D_P , (top) and T_{2B} , T_{2P} (bottom) for methane as a function of pressure. Note that the Mod D_B curves for SS and LS are the same.

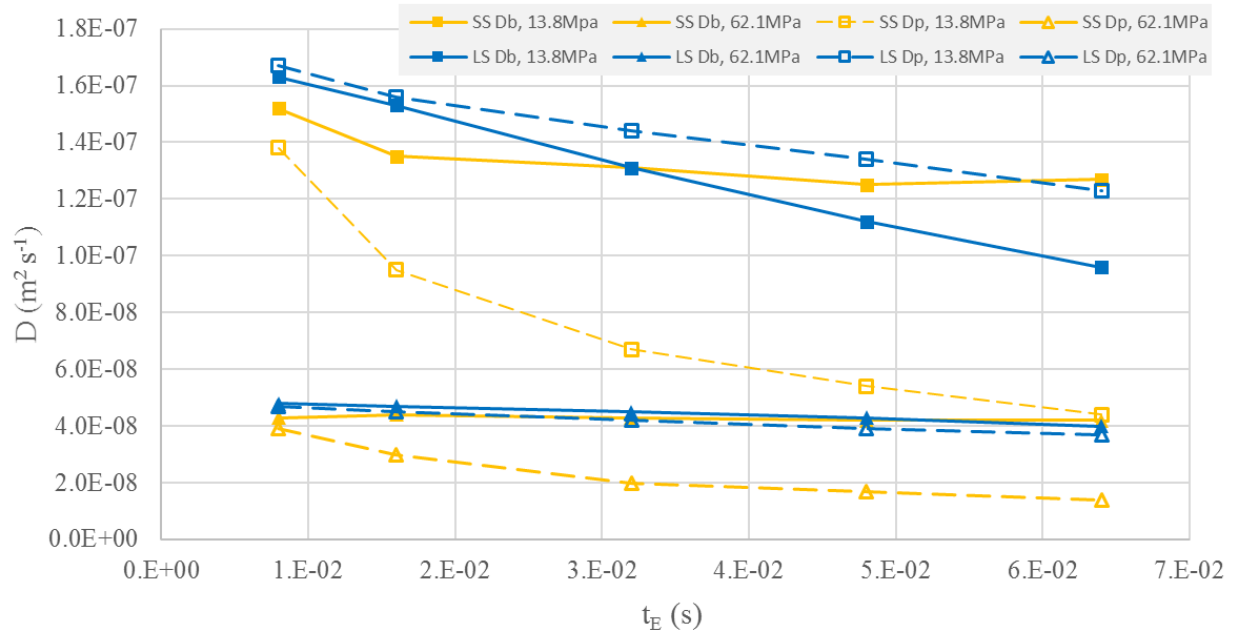


Figure 3 – Variation in experimental D_B and D_P as a function of t_E .